

# Origins of high $Q$ on microwave tungstenbronze-type like $\text{Ba}_{6-3x}\text{R}_{8+2x}\text{Ti}_{18}\text{O}_{54}$ ( $R$ : rare earth) dielectrics based on the atomic arrangements

Hitoshi Ohsato\*

*Material Science and Engineering, Nagoya Institute of Technology, Gokiso-cho, Showa-ku, Nagoya 466-8555, Japan*

## Abstract

Microwave dielectrics are key materials for wireless communications, which have been tremendously developed in ubiquitous age. On the microwave dielectrics, there are three important properties, such as quality factor  $Q$ , dielectric constants  $\epsilon_r$  and temperature coefficients of resonant frequency  $\tau_f$ . The utilizable region for the frequency is expanding to higher frequency. Since the dielectric losses increase at higher frequencies, microwave dielectrics with high quality factor  $Q$  are of considerable interest. In this paper, we research the origin of high  $Q$  for the next generation dielectrics. We summarize the cases with high  $Q$  and state the origin of high  $Q$  on the tungstenbronze-type like solid solutions, which we have studied. © 2006 Elsevier Ltd. All rights reserved.

**Keywords:** Tungstenbronze-type compound; Impurities; Dielectric properties

## 1. Introduction

The wireless communications have been tremendously developed in the following applications: portable telephone, satellite broadcasting, ultra-high speed wireless LAN, intelligent transport system (ITS) including ETC and ladder for anti-collision, and so on. The utilizable region for the frequency is expanding to millimeter wave region because of shortage of the radio frequency (rf) resource. Usually, in the high frequency region, the dielectric losses increase. So, the developments of microwave dielectrics with the high quality factor  $Q$ , which is the inverse of  $\tan \delta$  are expected. We have been studying the tungstenbronze-type like  $\text{Ba}_{6-3x}\text{R}_{8+2x}\text{Ti}_{18}\text{O}_{54}$  ( $R$ : rare earth) solid solutions with high  $Q$  and high  $\epsilon_r$  and low temperature coefficient of frequency  $\tau_f$ , and published many papers.<sup>1–8</sup> These compounds are located on the tie-line between  $\text{BaTiO}_3$ – $\text{R}_2\text{Ti}_3\text{O}_9$  compositions in the  $\text{BaO}$ – $\text{R}_2\text{O}_3$ – $\text{TiO}_2$  ternary system.  $\text{Ba}_{6-3x}\text{R}_{8+2x}\text{Ti}_{18}\text{O}_{54}$  solid solutions<sup>3</sup> have a tungstenbronze-type like structure as shown in Fig. 1. The crystal data with superlattice doubled of  $c$ -axis are as follows: orthorhombic  $Pbnm$  (no. 62),  $a = 12.13 \text{ \AA}$ ,  $b = 22.27 \text{ \AA}$ ,  $c = 7.64 \text{ \AA}$  and  $Z = 2^2$ . The fundamental unit cell of the structure contains three types of large cation sites: ten A1-

rhombic sites in  $2 \times 2$  perovskite blocks, four A2-pentagonal sites and four C-trigonal sites.<sup>4</sup> The pentagonal and trigonal sites are located among the perovskite blocks. The fundamental structure is expressed by the formula  $[\text{R}_{8+2x}\text{Ba}_{2-3x}\text{V}_x]_{\text{A1}}[\text{Ba}_4]_{\text{A2}}[\text{V}_4]_{\text{C}}\text{Ti}_{18}\text{O}_{54}$  ( $0 \leq x \leq 2/3$ ). Here, V means vacancy. In the  $0 \leq x < 2/3$  composition region, the A1-sites are occupied mainly by medium-sized  $R$ -ions, and also by a small amount of large Ba-ions. For  $x = 2/3$ , the A1- and A2-sites are occupied by  $R$ - and Ba-ions, respectively. On the other hand, the C-sites are unoccupied by cations, because they are the smallest sites.

The coordination numbers CN and configurations of each polyhedron in the tungstenbronze-type like  $\text{Ba}_{6-3x}\text{R}_{8+2x}\text{Ti}_{18}\text{O}_{54}$  crystal structures are illustrated in a previous paper.<sup>5</sup> A1(1)- and A1(5)-sites are two-cap trigonal prisms with 8-CN, A1(2)- and A1(4)-sites are a distorted cubic dodecahedra with 8-CN, and the A1(3)-site is a three-cap trigonal prism with 9-CN, whereas A2(1)- and A2(2)-sites are a two-cap hexahedron with 10-CN. The configurations of C-sites have not been determined yet because crystal structure analysis showed that C-site is unoccupied.

In this paper, cases with high  $Q$  on the tungstenbronze-type like  $\text{Ba}_{6-3x}\text{R}_{8+2x}\text{Ti}_{18}\text{O}_{54}$  solid solutions are summarized as following three cases. Case 1: quality factor improved by compositional ordering.<sup>6–8</sup> Case 2:  $Q$  improved by more compositional ordering.<sup>9–11</sup> Case 3: quality factor depending on  $R$ -cations.<sup>12</sup>

\* Tel.: +81 52 735 5284; fax: +81 52 735 5284.  
E-mail address: [ohsato.hitoshi@nitech.ac.jp](mailto:ohsato.hitoshi@nitech.ac.jp).

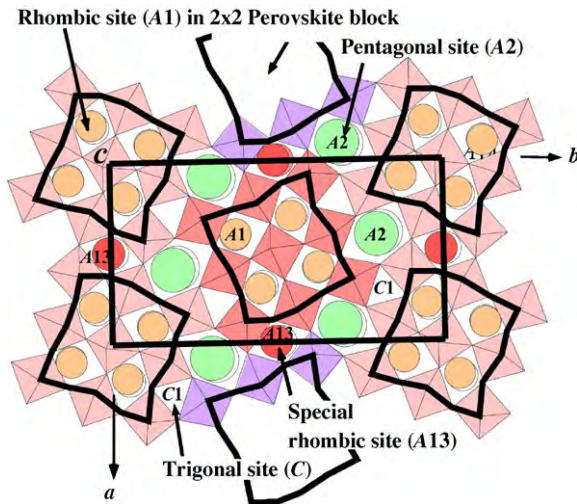


Fig. 1. Crystal structure of the tungstenbronze-type like  $\text{Ba}_{6-3x}\text{R}_{8+2x}\text{Ti}_{18}\text{O}_{54}$  solid solutions.

Moreover, the origins of  $Q$  are considered based on these three cases.

## 2. Experiments

The experimental procedure for synthesis of samples, identification of precipitated phases, measurement of stress and properties and crystal structure analysis are described in our previous papers.<sup>1–8</sup>

The stability of crystal structure was discussed by using bond valence theory<sup>13–15</sup> to clarify the relationship between the differences in the ionic radii of cations and the crystal structure. Salinas-Sanchez et al.<sup>16</sup> reported the stability index of the crystal structure which related with the difference in the valence calculated from the bond valence theorem and the theoretical valence. Thus, in this study, the bond valence  $v_i$  of specific cation in the crystal structure was evaluated by the following equations:

$$S_{ij} = \exp \frac{R_0 - R_{ij}}{b} \quad (1)$$

$$v_i = \sum_j S_{ij} \quad (2)$$

where  $S_{ij}$  represents the bond strength of cation  $i$  and anion  $j$ ;  $R_{ij}$  bond length between  $i$  and  $j$ ;  $R_0$  and  $b$  are known as the bond valence parameters of various cations and the constant value (0.37 Å), respectively.

## 3. Results and discussions

### 3.1. Improvement of $Q$

#### 3.1.1. Case 1: compositional ordering<sup>6–8</sup>

We found that  $Qf$  values have non-linearity as a function of composition in a tungstenbronze-type like  $\text{Ba}_{6-3x}\text{R}_{8+2x}\text{Ti}_{18}\text{O}_{54}$  ( $R$ : rare earth) solid solutions as shown in Fig. 2. The solid solutions are superior compounds having high  $\epsilon_r$  and high  $Qf$  for mobile phone, and have the highest  $Qf$  value at  $x=2/3$  com-

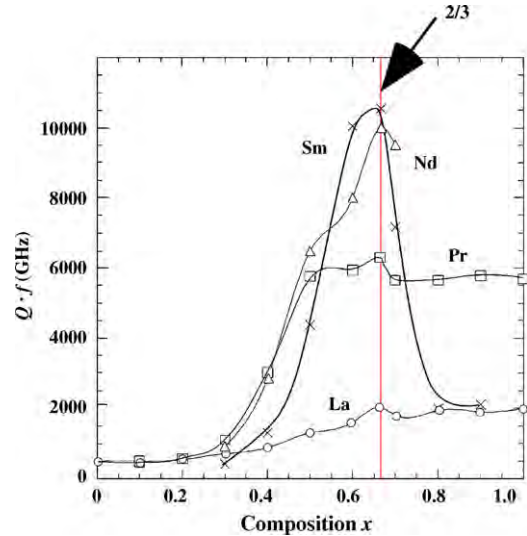


Fig. 2. Quality factor of the tungstenbronze-type like  $\text{Ba}_{6-3x}\text{R}_{8+2x}\text{Ti}_{18}\text{O}_{54}$  solid solutions as a function of composition.

position: 10549 GHz in the Sm system, 10010 GHz in the Nd system and 2024 GHz in the La system.<sup>4</sup> The highest quality factor is based on the compositional ordering of  $R$ - and Ba-ions in the rhombic A1- and pentagonal A2-sites, respectively, as shown in Fig. 3. The highest quality factor may be based on the ordering of  $R$ - and Ba-ions in the rhombic A1- and pentagonal A2-sites, respectively. The distribution of the ions might reduce the internal strain and result in the non-linear variation of quality factor.

#### 3.1.2. Case 2: more compositional ordering<sup>9–11</sup>

Sr-ions with ionic size between that of Ba- and  $R$ -ions are introduced in to this system, of which ionic size is located between Ba- and  $R$ -ions. As mentioned above,  $Qf$  values of

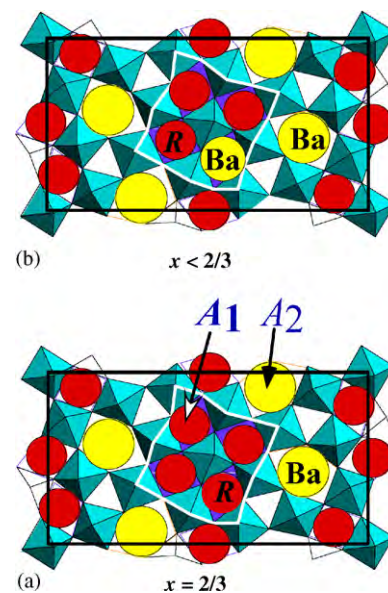


Fig. 3. In the case of just  $x=2/3$  (a), compositional ordering at A1- and A2-sites by  $R$ - and Ba-ions, respectively. In the case of  $x < 2/3$  (b), Ba-ions also occupy A1-sites statistically.

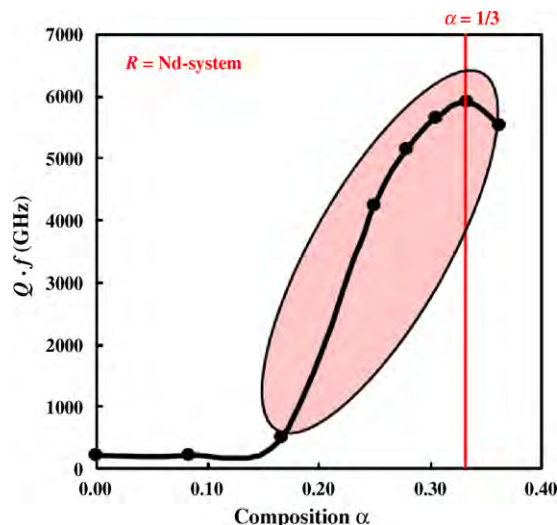


Fig. 4.  $Qf$  values as a function of  $\alpha$  on the  $(\text{Ba}_{1-\alpha}\text{Sr}_\alpha)_6\text{R}_8\text{Ti}_{18}\text{O}_{54}$  with  $x=0$ . The values are increased steeply by substitution Sr- for Ba-ions.

those  $\text{Ba}_{6-3x}\text{R}_{8+2x}\text{Ti}_{18}\text{O}_{56}$  solid solutions have the maximum value at  $x=2/3$ . In the region  $x < 2/3$ , the structural formula of the solid solutions is  $[\text{R}_{8+2x}\text{Ba}_{2-3x}\text{V}_x]_{\text{A1}}[\text{Ba}_4]_{\text{A2}}\text{Ti}_{18}\text{O}_{54}$ . In this region, Ba-ions located in A1-sites deteriorate the quality factor. In the case of  $x=0$ ,  $Qf$  values are very low as shown in Fig. 2. When Ba-ions are substituted by Sr-ions, such as  $[\text{R}_8\text{Sr}_2]_{\text{A1}}[\text{Ba}_4]_{\text{A2}}\text{Ti}_{18}\text{O}_{54}$ ,  $Qf$  values are improved steeply from 206 to 5880 GHz in the case of  $R=\text{Nd}$  as shown in Fig. 4. Introduction of Sr-ions in A1-sites may reduce the internal stress/fluctuation of  $d$ -spacing, because of reducing ionic size in A1-sites. Mercurio et al.<sup>11</sup> reported that the Sr-ions occupy in A13 special sites which have medium size between that of A1- and A2-sites. Hence, it is expected that R-, Sr- and Ba-ions are ordering in A1-, A13- and A2-sites, respectively.

### 3.1.3. Case 3: dependence of $Qf$ on R-cation with small size<sup>12</sup>

The quality factors  $Qf$  of each R-analogy with  $x=2/3$  are shown as a function of ionic radius in Fig. 5. It should be noticed that the quality factors  $Qf$  increase with the decrease of the ionic

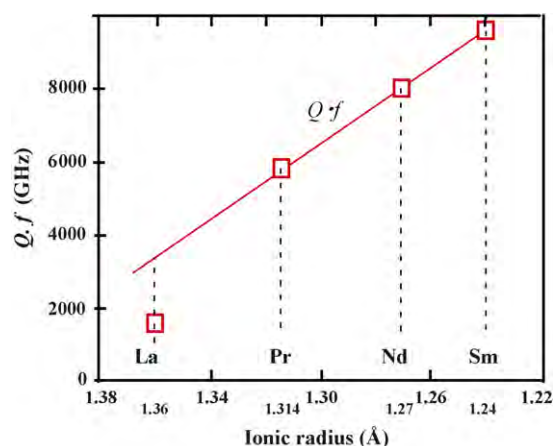
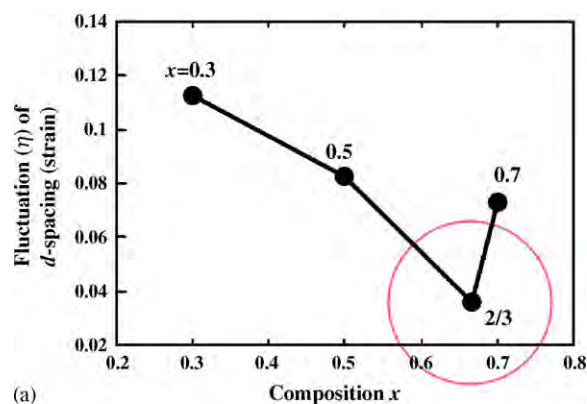
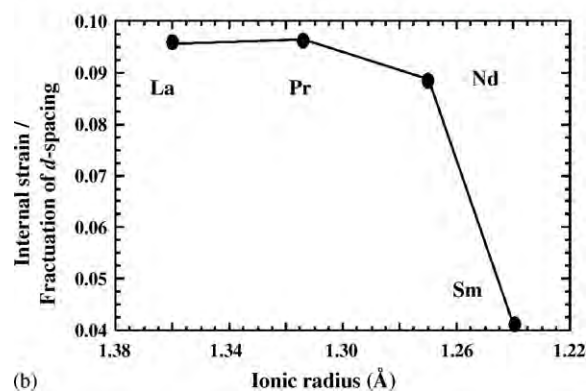


Fig. 5. Dependence of quality factor on the R-ions.



(a)



(b)

Fig. 6. Dependence of internal strain on the composition  $x$  (a) and R-ions (b).

radii of each R-ion as described later. The  $Qf$  values of Sm- and Nd-analogies are excellent. The  $Qf$  of Sm-analogy is the highest due to the low internal strain/fluctuation of  $d$ -spacing on the atomic scale as shown in Fig. 6(b). It should be noticed that internal strain  $\eta$  for Sm is the lowest. This low  $\eta$  originates from the difference of ionic radii between R- and Ba-ions. In the case of  $\text{Ba}_{6-3x}\text{R}_{8+2x}\text{Ti}_{18}\text{O}_{54}$  solid solution series, lower internal strain/fluctuation of  $d$ -spacing originate from the ordering of R- and Ba-ions that occupy A1- and A2-sites, respectively. In the case of R-analogies with  $x=2/3$ , we are comparing R-analogies with different size of ionic radii. The tungstenbronze-type like structure is built with two different parts. One is perovskite blocks, which include medium size ions, such as R-ions, and another is pentagonal columns, which include large size ions, such as Ba-ion. These two parts are produced by existence of different size in cations. Therefore, the size of cations occupying the two sites should be different. Sm-analogy with the smallest ionic radius in the R-analogous series is the most stable for the rhombic A1-sites in the perovskite blocks, which show the smallest internal strain. This stabilization of the crystal structure has improved  $Qf$  values.

### 3.2. Origin of $Q$

We would like to consider the origin of the high  $Q$  on the three cases described above. There are three structurally different aspects: first one is different ionic size of Ba- and R-cations, second one is substitution between cations with different charge, and third one is the formation of polars.



### 3.2.1. Internal strain

As ionic radius<sup>17</sup> of Ba-ion with 1.42 Å (8-CN) is larger than that of *R*-ion (Sm/Nd) with 1.1 Å (8-CN) as mentioned in the second case, Ba-ions with large ionic size in perovskite block bring deformation of crystal structure and internal strain in the range of  $0 \leq x < 2/3$ , as shown in Fig. 6(a). It should be noticed that the internal strain for  $x=2/3$  is the lowest in the series of  $\text{Ba}_{6-3x}\text{Sm}_{8+2x}\text{Ti}_{18}\text{O}_{54}$  solid solutions.<sup>8</sup> This low internal strain comes from the distribution of cations in the rhombic sites and the pentagonal sites on the tungstenbronze-type like structure. As shown before in the  $x=2/3$  composition, ions with the same size occupy each A1- and A2-site, as shown in the structural formula  $[\text{R}_{9.33}\text{V}_{0.67}]_{\text{A1}}[\text{Ba}_4]_{\text{A2}}\text{Ti}_{18}\text{O}_{54}$ , that means, *R*-ions and Ba-ions are ordering in both the rhombic sites and pentagonal sites, respectively. This ordering leads to the lowest strain. As the  $x$ -values decrease according to the structural formula  $[\text{R}_{8+2x}\text{Ba}_{2-3x}\text{V}_x]_{\text{A1}}[\text{Ba}_4]_{\text{A2}}\text{Ti}_{18}\text{O}_{54}$  in the range of  $0 \leq x < 2/3$ , Ba-ions with larger ionic radii will occupy also a part of the rhombic sites with their smaller size. The occupation of Ba-ions in A1-site leads to internal strain around themselves, which lowers the *Qf* values. The strain is based on the fluctuation of *d*-spacing.

### 3.2.2. Substitution between cations with different charge

As mentioned in the first case, trivalent cation in the perovskite block brings stability of crystal structure, which can be discussed by using bond valence theory. The bond valences of Sm- and Nd-analogies with  $x=0.5$  and  $0.7$  are calculated from refined atomic position reported in a previous paper.<sup>1</sup> Though ideal coordination numbers are 12-CN in A1-sites and 15-CN in A2-sites, the real coordination number is 8-CN in A1-sites in perovskite block and one of A1-sites is 9-CN because of deformation of these polyhedra as describe before. The coordination number was fixed at 8 for A1-sites and 10 for A2-sites. The bond valence parameters of  $R_0$  relate to  $\text{Ba}_{6-3x}\text{R}_{8+2x}\text{Ti}_{18}\text{O}_{54}$  are listed in Table 1.  $R_{ij}$  was obtained from the reported atomic position of the crystal structural refinement.<sup>1</sup> Bond valences  $\nu$  of cation are summarized  $s_{ij}$  bond strengths.  $\nu$  of Ba in A1-site on  $x=0.5$  composition is 4.07 and 4.57 for Nd- and Sm-analogy which value is far exceed  $2^+$  divalent of Ba. On the other hand,  $\nu$ -values of rare-earth ions in A1-sites are fitting with  $3^+$  trivalent ions. So, Ba-ions in A1-sites are unstable and bring large losses. In the case of  $x=0.7$ , all the  $\nu$ -values are fitting with the cation valence.

### 3.2.3. Formation of polars

As mentioned in the first case, on the Sm-analogy with  $x=0.5$  composition smaller than  $x=2/3$ , Ba-ions in A1-sites have large

Table 2

Bond valences of  $\text{Ba}_{6-3x}\text{R}_{8+2x}\text{Ti}_{18}\text{O}_{54}$  obtained from refined atomic position

<i>R</i>	<i>x</i>	$\langle \nu_{\text{A1-R}} \rangle$	$\langle \nu_{\text{A1-Ba}} \rangle$	$\langle \nu_{\text{A2}} \rangle$	$\langle \nu_{\text{Ti}} \rangle$
Nd	0.5	2.57	4.07	1.94	4.09
	0.7	2.71	—	2.00	4.11
Sm	0.5	2.73	4.57	2.01	4.13
	0.7	2.93	—	2.07	4.15

Coordination number was fixed at 10 for Ba in A2-site, 6 for Ti in B-site and, 8 and 9 for A1-site.

bond valences of 4.57 (Table 2) which are lack of charge by about +2. The lack shows unbalance of the charge valence, which makes polars between the Ba positions and oxygen. Other bond valences of Ba in A2-sites and Ti in B-sites are 2.01 and 4.13 almost similar  $2^+$  and  $4^+$  valence, respectively, though that of Sm is 2.71 a little different from  $3^+$ . In the case of  $x=0.7$  composition on the Sm-analogy, the bond valence of Ba in A1-sites is improved to 2.93 which is close to  $3^+$ . In the case of Nd-analogy with  $x=0.7$ , the bond balance of *R*-ions is a little degraded to 2.71. So, the *Q* is also a little degraded as mentioned in the third case. On the other hand, vacancies in A1-sites on the structural formula  $[\text{R}_{8+2x}\text{Ba}_{2-3x}\text{V}_x]_{\text{A1}}[\text{Ba}_4]_{\text{A2}}\text{Ti}_{18}\text{O}_{54}$  are created by the substitution of  $2R$  for  $3Ba$  in the solid solutions. Though vacancies are increased according to  $x$ , *Q* also increases steeply as shown in Fig. 4. These vacancies work for stability of the crystal structure, because the vacancies reduce the site volume. In this tungstenbronze-type structure, two differently sized cations, such as *R* and Ba can be included in two differently sized polyhedra: rhombic A1-site and pentagonal A2-site. Here, A1-site is deformed from cuboctahedron to form a rhombohedron to reduce the site volume. However, effects of the vacancies for creation of polars are not so clearly.

## 4. Conclusions

We summarized three cases for improvement of *Q* on the tungstenbronze-type like  $\text{Ba}_{6-3x}\text{R}_{8+2x}\text{Ti}_{18}\text{O}_{54}$  solid solutions: first case is compositional ordering at  $x=2/3$  which composed by the rhombic sites in the perovskite blocks and pentagonal sites occupied by *R* and Ba, respectively. Second case is more improvement of *Q*, which is achieved by the substitution of medium sized Sr-ions (between Ba- and *R*-ions) for Ba-ions. The third case is improvement *Q* depending on *R*-cations. In the case of Sm-ions with small ionic size, a high *Qf* is observed. We have also considered three origins of high *Q* on the three cases described above, i.e. dependence of internal strain on the ionic size, stability of crystal structure depends on the charge valences and the formation of polars which degrade *Q*.

## Acknowledgements

This report is depend on the many researches, so I thanks all authors appeared on the reference concerning this paper. A part of this study was supported by following projects on Japanese Ministry of Education, Science and Culture and

Table 1  
Parameter  $R_0$  values in the bond valence theorem

Bond	$R_0$
$\text{Ba}^{2+}-\text{O}$	2.285
$\text{Nd}^{3+}-\text{O}$	2.105
$\text{Sm}^{3+}-\text{O}$	2.088
$\text{Ti}^{4+}-\text{O}$	1.815

by NEDO foundation for matching fund: a Grant-in Aid for Science Research (B) supported, the NITECH 21st Century COE program “World Ceramics Center for Environmental Harmony”, and “NIT-Seto Ceramics R&D Project”.

## References

- Ohsato, H., Science of tungstenbronze-type like  $\text{Ba}_{6-3x}\text{R}_{8+2x}\text{Ti}_{18}\text{O}_{54}$  (R: rare earth) microwave dielectric solid solutions. *J. Eur. Ceram. Soc.*, 2001, **21**, 2703–2711.
- Ohsato, H., Nishigaki, S. and Okuda, T., Superlattice and dielectric properties of dielectric compounds. *Jpn. J. Appl. Phys.*, 1992, **31**(9B), 3136–3138.
- Ohsato, H., Ohhashi, T., Nishigaki, S., Okuda, T., Sumiya, T. and Suzuki, S., Formation of solid solutions of new tungsten bronze-type microwave dielectric compounds  $\text{Ba}_{6-3x}\text{R}_{8+2x}\text{Ti}_{18}\text{O}_{54}$  (R = Nd and Sm,  $0 < x < 1$ ). *Jpn. J. Appl. Phys.*, 1993, **32**(9B), 4324–4326.
- Ohsato, H., Ohhashi, T., Kato, H., Nishigaki, S. and Okuda, T., Microwave dielectric properties and structure of the  $\text{Ba}_{6-3x}\text{Sm}_{8+2x}\text{Ti}_{18}\text{O}_{54}$  solid solutions. *Jpn. J. Appl. Phys.*, 1995, **34**, 187–191.
- Ohsato, H., Futamata, Y., Sakashita, H., Araki, N., Kakimoto, K. and Nishigaki, S., Configuration and coordination number of cation polyhedra of tungstenbronze-type-like  $\text{Ba}_{6-3x}\text{Sm}_{8+2x}\text{Ti}_{18}\text{O}_{54}$  solid solutions. *J. Eur. Ceram. Soc.*, 2003, **23**, 2529–2533.
- Ohsato, H., Mizuta, M., Ikoma, T., Onogi, Y., Nishigaki, S. and Okuda, T., Microwave dielectric properties of tungsten bronze-type  $\text{Ba}_{6-3x}\text{R}_{8+2x}\text{Ti}_{18}\text{O}_{54}$  (R = La, Pr, Nd and Sm) solid solutions. *J. Jpn. Ceram. Soc.*, 1998, **106**, 178–182.
- Ohsato, H., Imaeda, M., Komura, A. and Okuda, T., Non-linear microwave quality factor change based on the site occupancy of cations on the tungstenbronze-type  $\text{Ba}_{6-3x}\text{R}_{8+2x}\text{Ti}_{18}\text{O}_{54}$  (R: rare earth) solid solutions. In *Proceeding of the International Symposium on Dielectric Ceramics*, 1998; Nair, K. M. and Bhalla, A. S. ed., *Dielectric Ceramic Materials*, Ceramic Transaction, vol. 100. The American Ceramic Society, Westerville, Ohio 43081, 1998, pp. 41–50.
- Ohsato, H., Imaeda, M., Takagi, Y., Komura, A. and Okuda, T., Microwave quality factor improved by ordering of Ba and rare-earth on the tungstenbronze-type  $\text{Ba}_{6-3x}\text{R}_{8+2x}\text{Ti}_{18}\text{O}_{54}$  (R = La, Nd and Sm) solid solutions. In *Proceeding of the XIth IEEE International Symposium on Applications of Ferroelectrics*, 1998, pp. 509–512 [IEEE catalog number 98CH36245].
- Nagatomo, T., Otagiri, T., Suzuki, M. and Ohsato, H., Microwave dielectric properties and crystal structure of the tungstenbronze-Type Like  $(\text{Ba}_{1-\alpha}\text{Sr}_{\alpha})_6(\text{Nd}_{1-\beta}\text{Y}_{\beta})_8\text{Ti}_{18}\text{O}_{54}$  solid solutions. *J. Eur. Ceram. Soc.*, 2006, **26**, 1895–1898.
- Imaeda, M., Mizuta, M., Ito, K., Ohsato, H., Nishigaki, S. and Okuda, T., Microwave dielectric properties of  $\text{Ba}_{6-3x}\text{R}_{8+2x}\text{Ti}_{18}\text{O}_{54}$  solid solutions substituted Sr for Ba. *Jpn. J. Appl. Phys.*, 1997, **36**(9B), 6012–6015.
- Mercurio, D., Abou-Salama, M. and Mercurio, J.-P., Investigations of the tungstenbronze-type  $(\text{Ba}_{1-\alpha}\text{Sr}_{\alpha})_{6-x}\text{La}_{8+2x/3}\text{Ti}_{18}\text{O}_{54}$  ( $0 \leq x \leq 3$ ) solid solutions. *J. Eur. Ceram. Soc.*, 2001, **21**, 2713–2716.
- Ohsato, H., Mizuta, M. and Okuda, T., Crystal structure and microwave dielectric properties of tungstenbronze-type  $\text{Ba}_{6-3x}\text{R}_{8+2x}\text{Ti}_{18}\text{O}_{54}$  (R = La, Pr, Nd and Sm) solid solutions. In *Proceeding of the XVII Conference, Applied Crystallography*, 1997, pp. 440–447.
- Brown, I. D., Empirical parameters for calculating cation-oxygen bond valences. *Acta Cryst.*, 1973, **A29**, 266–282.
- Brown, I. D., Empirical bond-strength–bond-length curves for oxides. *Acta Cryst.*, 1973, **B32**, 1957–1959.
- Brown, I. D., Bond-valence parameters from a symmetric analysis of the inorganic crystal structure database. *Acta Cryst.*, 1985, **B41**, 244–247.
- Salinas-Sanchez, A., Grancia-Munoz, J. L., Rodriguez-Carvajal, J., Saez-Puche, R. and Martinez, J. L., Structural characterization of  $\text{R}_2\text{BaCuO}_5$  (R = Y, Lu, Tm, Er, Ho, Dy, Gd, Eu and Sm) oxides by X-ray and neutron diffraction. *J. Solid State Chem.*, 1992, **100**, 201–211.
- Shannon, R. D., Dielectric polarizabilities of ions in oxides and fluorides. *J. Appl. Phys.*, 1993, **73**, 348–366.